Received: 23 May 2025 | Revised: 19 September 2025 | Accepted: 7 October 2025

DOI: 10.1002/dep2.70051

The Depositional Record Open Access
A journal of the International Association of Sedimentologists
WILEY

METHOD

Taking machine learning with a grain of sand: Sediment Analysis Neural-network Data-engine (SAND-e) reveals sedimentological differences between turbid and clear-water reefs

G. William M. Harrison[1,2] | **Teigan G. Collins**[3,4] | **Allia Rosedy**[5] | **Nadia Santodomingo**[3,6] | **Willem Renema**[1,2] | **Kenneth G. Johnson**[3]

[1]Naturalis Biodiversity Center, Leiden, The Netherlands

[2]University of Amsterdam, Amsterdam, The Netherlands

[3]Natural History Museum (London), London, UK

[4]Imperial College London, London, UK

[5]Universiti Malaysia Sabah, Kota Kinabalu, Malaysia

[6]Senckenberg Research Institute and Natural History Museum, Frankfurt, Germany

Correspondence
G. William M. Harrison, Naturalis Biodiversity Center, Leiden, The Netherlands.
Email: william.harrison@naturalis.nl

Funding information
Natural Environment Research Council, Grant/Award Number: NE/R011044/1; H2020 Marie Skłodowska-Curie Actions, Grant/Award Number: 813360; Universiti Malaysia Sabah, Grant/Award Number: GUG0415-2/2019

Abstract

Sediment is an important facet of sand cay reefs as it is responsible for reef accretion and island formation, with shifts in the proportions of sediment producers being proxies for ecological shifts. However, manual sediment analyses require experts to identify thousands of sand grains by hand before beginning data analysis. To accelerate the process, we developed the Sediment Analysis Neural-network Data-engine (SAND-e) to estimate the proportions of sediment producers, based on segmentation and classification of carbonate sand grains from microscope camera imagery. Sediment from Darvel Bay was used for training due to the variability of sand cay reefs available in that area. SAND-e segmented 1686 images into 32 883 grains within 3.5 h. The grains were then fed through SAND-e's classifier ensemble, containing four classifiers that voted to classify the grains into one of five classes (calcareous algae, coral, foraminifera, molluscs and 'other') in 1 hour. Both SAND-e and 11 humans annotated grains from the same dataset to ensure that SAND-e's accuracy was within the already accepted error rate deriving from multiple human annotators.

KEYWORDS

carbonate producers, coral reef, coral triangle, machine learning

1 | INTRODUCTION

Coral reefs are extraordinarily diverse and highly important marine ecosystems contributing to a wide range of goods and services such as tourism, coastal protection, food and the provision of natural products and livelihood to millions of people (Moberg & Folke, 1999). One of these critical functions is carbonate sediment production, in which the dead shells,

G. William M. Harrison and Teigan G. Collins share first authorship.

skeletons and tests of reef-dwelling creatures such as algae, corals and molluscs sustain the reef morphology and build low-lying islands (Kappelmann et al., 2023). However, this important ecosystem service provided by coral reefs is threatened (De'ath et al., 2009). As global temperatures continue to rise, coral reefs are experiencing mass bleaching events (Hoegh-Guldberg, 1999) with increasing intensity and frequency, resulting in the mass death of reef corals and potentially reducing their active role in sediment production (Lange et al., 2024).

Sediment production is an ecosystem service provided by coral reefs and an important component of reef carbonate budgets. Biogenic carbonate production occurs both on a framework level (e.g. corals, large molluscs, CCA) and through direct sediment production (e.g. foraminifera, micro-molluscs, *Halimeda*) (Perry et al., 2023). Framework components can enter the sediment fraction by mechanical or biological erosion (Perry et al., 2023). Additionally, sediment is frequently transported off the reef and onto the slope (Kappelmann et al., 2023). While on-reef sediment mainly fills the space between corals in framework reefs (Brown et al., 2021), it is what sustains the morphology of sand cay reefs, providing benefits such as continued reef island building (McKoy et al., 2010; Woodroffe & Morrison, 2001; Woodroffe et al., 2007). The latter is particularly important in regions where reef islands are inhabited in times of rising sea level.

Furthermore, reef sediment from cores is often used as a proxy to reconstruct past conditions on a reef (Cramer et al., 2017; Johnson et al., 2017; O'Dea et al., 2020) despite taphonomic biases (Hausmann et al., 2018; Kosnik et al., 2009; Zuschin et al., 2000). Comparisons with modern sediment allow researchers to detect ecological baseline shifts that occurred before monitoring began (Cramer et al., 2017; Johnson et al., 2017; O'Dea et al., 2020). While some studies survey living organisms on a reef to estimate overall carbonate production (Lange et al., 2024; Perry et al., 2018; Perry et al., 2023), direct analysis of the sediments is needed to determine how much of the gross carbonate ends up in the sediment and contributes to reef accretion and island building.

Manual sediment analyses are time-consuming because they require an expert to identify at least 200 sediment grains (Kappelmann et al., 2023; Janßen et al., 2017; Morgan & Kench, 2016; Cuttler et al., 2019; Bonesso et al., 2022) or 400-point counts (McKoy et al., 2010) per site to achieve a crude categorical level. Therefore, we explored the capability of machine learning to accelerate the analysis of grain composition in reef sediments. Ecologists and sedimentologists have used images from photographs, drawings and paintings to quantify processes like regime shifts, island building and predator–prey dynamics in a relatively slow and low-throughput method for many years (Kappelmann et al., 2023; Laux et al., 2022; Roelfsema et al., 2006). However, modern digitalisation techniques have allowed for image collection speeds to progress at an ever-increasing rate and frequently can outpace the capacity to manually extract meaningful data from images (Lürig et al., 2021; Marchant et al., 2020; Mimura et al., 2022). Machine learning (ML), a form of artificial intelligence (AI), has been applied in many Earth Sciences domains such as land use estimation (Jin et al., 2019), crop yield prediction (Jin et al., 2019) and ocean current modelling (Sinha & Abernathey, 2021). Machine learning uses a bottom-up approach in which algorithms learn relationships between input data and output results as part of the model-building effort and can discover patterns and trends buried within vast volumes of data that are not apparent to human analysts. Computer vision (CV), the automated extraction and processing of information from digital images, provides an opportunity to alleviate the longstanding bottleneck with the capability to be an efficient and comprehensive data extraction technique (Lürig et al., 2021; Marchant et al., 2020; Mimura et al., 2022). Recent examples of successful ecological applications were published by Porto and Voje (2020) in which biological structures in images of fly wings, sea basses and bryozoan colonies were automatically detected and landmarked, finding that the time–weight performance of annotation was massively advantaged compared to manual annotation but also describes boundaries to these machine learning models, such as limitations to 2D images. Machine learning is already being applied to sedimentology. Automated sedimentological data generation has a long history, especially in siliciclastic environments (Butler et al., 2001), with models capable of automatically classifying sediment type and grain-size distributions available (Buscombe, 2020). More recently, segmenters have been developed for siliciclastic sediments. Segment Every Grain, an offshoot of the Segment Everything models, allows for one-click segmentation of siliciclastic grains from each other and a background (Sylvester, 2023). By contrast, GrainID allows for segmentation of fluvial sediments automatically while also measuring the size of the sediment grains (Mair et al., 2024). However, no machine learning-based tools have been developed to work with carbonate sediments.

Most of the existing understanding of the ecological function, diversity, and sedimentary development of coral reefs is based on data from clear-water settings, but there is increasing recognition of the importance of reefs in turbid, nearshore settings (Guest et al., 2012; Morgan et al., 2017; Anthony et al., 2007; Rosedy

et al., 2023, Santodomingo et al., 2016). Evidence of long-term persistence and resilience of turbid reefs comes from the fossil record (Santodomingo et al., 2016) and from the observed ability to reduce the impact or even escape the most recent bleaching events in 2010 (Guest et al., 2012), 2016–2017 (Morgan et al., 2017) and 2020–2021 (Rosedy et al., 2023; Zweifler et al., 2024). We ensure that our models can function on sediment from both habitat types by analysing nine sediment samples across three contrasting environments in Darvel Bay (Sabah, Malaysia): the clear-water reef of Blue Lagoon, the turbid Triangle Reef and the more turbid reef at Sakar North. The purpose is to demonstrate the applicability of machine learning in coral reef sedimentology by the following:

- Building an image set of sediment grains collected in three different environments.
- Training the Sediment Analysis Neural-network Data-engine (SAND-e) to segment and classify the main components.
- Using Darvel Bay as a test case to demonstrate the applicability of machine learning-based methods for analyses of reef sediments.

2 | METHODS

2.1 | Study Area

Darvel Bay is located on the eastern coast of Sabah, North Borneo, Malaysia. Three coral reef sites were selected based on their contrasting environmental conditions, particularly differences in turbidity, that is, the suspended sediment content, with Blue Lagoon representing the clear-water environment, Triangle Reef a moderate turbidity environment, Sakar North the very turbid-water environment (Figure 1). Sakar North is situated 280 m from shore and 5 km south of Lahad Datu, a city whose main economic activities are small-scale fisheries and oil palm plantations. Its high turbidity (6.28 NTU) comes from terrestrial runoff from the nearby Segama River and the coastal development of Lahad Datu (Rosedy et al., 2023). However, there is relatively high coral cover with healthy coral colonies (Figure 1E). In contrast, Blue Lagoon is a submerged semi-atoll reef located 13 km from the coast, in the middle of the bay and relatively away from coastal influence. Midday light availability is three orders of magnitude higher in Blue Lagoon than in Sakar North, while turbidity is very low (Rosedy et al., 2023). Finally, Triangle Reef is located 3.5 km from the coast and is thought to have 10 m LUX values between those of Blue Lagoon and Sakar North.

2.2 | Light Monitoring

HOBO Pendant® MX2202 loggers were placed at 10 m depth on all three reefs and measurements were taken every 5 min. The median LUX values between 10 am and 3 pm were calculated for each day and used to find the median, upper quantile and lower quantile for each reef. Data from October to November were used to calculate the dry season values and June was used for the wet season. All data were logged in 2019, which is the year sediment samples were taken. June was selected since it was the only month for which all HOBO loggers were functional; no dry season data could be recovered from the HOBO logger at Blue Lagoon in 2019.

2.3 | Sample Acquisition

During fieldwork carried out in April 2019, three seafloor samples of approximately 500 g were manually collected at each site at 10 m depth from Blue Lagoon (Sed46–48), Triangle (Sed22–24) and Sakar North (Sed37–39). Upon collection, samples were rinsed with fresh water and left in airtight containers for 24 h to allow fine sediments to settle. Water was then siphoned off each container and samples were air dried for another 24 hours. They were subsequently oven-dried at 120–150°C for 1 hour or until completely dried and kept in paper envelopes sealed inside airtight plastic bags. In the laboratory, samples were dry sieved into six fractions: <1.0 mm, 1.0–1.4 mm, 1.4–2.0 mm, 2.0–2.8 mm, 2.8–4.0 mm and >4.0 mm. Only the 1.0–1.4 mm (Fraction 1) and a further sieved fraction of 0.5–1.0 mm (Fraction 0.5) were used to create the image set. A breakdown of the images is shown in Table 1 These two size fractions were chosen because previous work on Blue Lagoon and Sakar North found that they are more abundant in sediment samples than the larger size fractions (Rosedy et al., 2023), both providing enough training data and saving more time by automating them. Previous surveys of sand cay reefs in the Coral Triangle found similar grain-size distributions (Janßen et al., 2017), suggesting that these models would be transferable to other studies. Smaller size fractions tend to contain vastly different unidentifiable biota, so they were excluded from the present study.

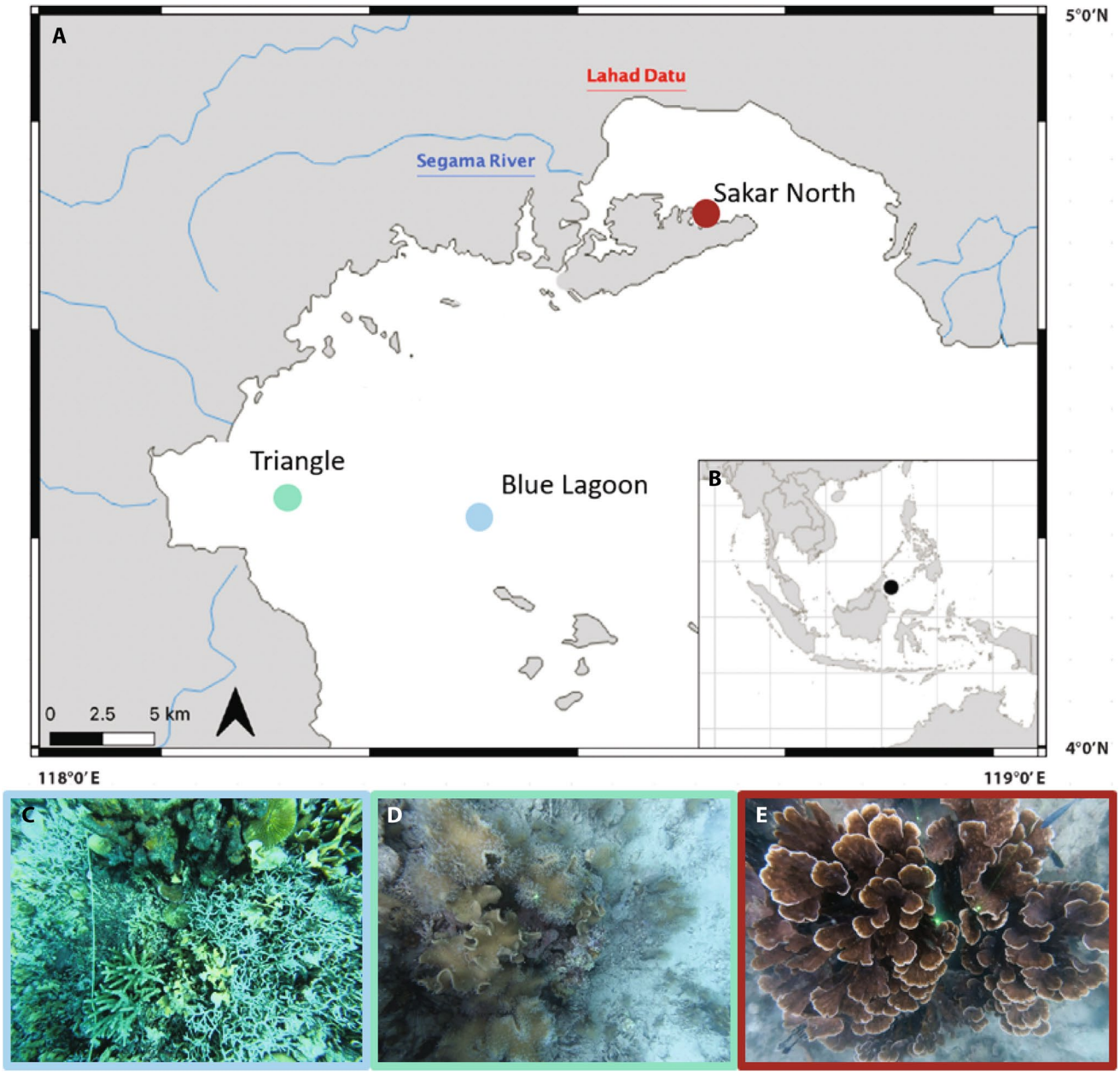

FIGURE 1 (A) Overview of Darvel Bay showing locations of the three reef environments (Blue Lagoon, Sakar North and Triangle), influential river systems and urban developments (B) Map of southeast Asia and the relative location of Darvel Bay (C–E) Imagery from the reef sites taken during sample collection at Blue Lagoon, Triangle and Sakar North, respectively.

2.4 | Sample Imaging

Grains from the six sediment samples were photographed to create an image set for both training the ML development tool and for analyses. Images were taken using an EOS 600D camera mounted on a Leica microscope and the following camera settings: ISO: 1/200, F:800, Size L, 1x magnification for optimum focus and highest pixel number (5184 × 3456). Between 6 and 56 sediment grains were individually arranged on the glass petri dish for imaging to limit the number of grains in contact and arrange for optimal grain numbers per image. A dark blue, untextured background was used to obtain high-contrast levels against the predominantly light-coloured grains.

We aimed at taking 50 images per size fraction per sample for the nine samples (Sed37-39, Sed22-24 and Sed46-48) and two size fractions of interest (Fraction 0.5 and Fraction 1), totalling 900 images. Some subsamples did not contain enough grains in certain fractions to make those targets, so others were imaged more intensively, both to compensate and due to extra available time. In total, 1676 images were taken (Figure 2A).

TABLE 1 Total images taken through microscope camera imagery, NHM Palaeontology Department October–November 2021, to build the imagery dataset from the nine samples across the three environments prior to upload into AI development tool. Fraction 1 = 1.0 mm to <1.4 mm, fraction 0.5 = 0.5 mm to <1.0 mm.

Locality	Sample no.	Fraction	Images
Blue Lagoon (BL)	Sed46	Fraction 1	229
		Fraction 0.5	90
	Sed47	Fraction 1	110
		Fraction 0.5	90
	Sed48	Fraction 1	40
		Fraction 0.5	58
Triangle (TR)	Sed22	Fraction 1	125
		Fraction 0.5	30
	Sed23	Fraction 1	105
		Fraction 0.5	75
	Sed24	Fraction 1	125
		Fraction 0.5	68
Sakar North (SN)	Sed37	Fraction 1	28
		Fraction 0.5	100
	Sed38	Fraction 1	162
		Fraction 0.5	122
	Sed39	Fraction 1	44
		Fraction 0.5	75

2.5 | Model training

Models were trained using the Geti AI development tool published by Intel (The Intel® Geti™ Platform, 2023). This platform modifies the weights on a deep convolutional neural network in order to minimise a loss function between the machine outputs and the example dataset. The task chain within the machine learning tool consisted of two phases: to segment grains within an image, 'Segmentation', and to classify the segmented grains using labels, 'Classification' (Figure 2B). As the ML development tool is reliant on user annotations of grains, where annotations are assumed to be of 100% confidence during training, it is important to classify grains into the class of labels for which the identification of the grain can be certain. A total of 596 images were annotated in a segmenter that used transfer learning protocols on the MaskRCNN-ResNet50 model architecture. Once the segmenter had enough annotations, Geti would begin making predictions of the grain boundary. Once those were acceptably accurate, we were able to focus entirely on training the classifier. Images from Sakar North and Blue Lagoon were used for this training set, as preliminary observations showed that they contain a higher diversity of grains in comparison to the other localities. In order to train the classifier, 1210 grains from 600 images were sorted into nine classes (bivalve, bryozoan, calcareous algae, coral, echinoderm, foraminifera, gastropod, silt-clay lump and unidentified molluscs). *Halimeda* and coralline algae were merged into one category due to the paucity of *Halimeda* in the samples; fewer than 10 *Halimeda* grains were identified. The entire image set and its greyscale counterparts were used to train four models. Two models used transfer learning from EfficientNet V2S and two used EfficientNet B0 as their basis. Models were further split based on the number of classes used. When training 'mollusc split' models, the gastropod and bivalve classes were kept separate and the unidentified mollusc class was excluded; bivalve and gastropod identifications were later combined to form the mollusc class. In contrast, the gastropod, bivalve and unidentified mollusc classes were combined into a single mollusc class in 'mollusc united' models. All four models were further trained on sediments from the islands of Kudingareng Keke and Samalona near Makassar, South Sulawesi, Indonesia that had not been dried in such hot conditions; these sediments came from the 0.5- to 2.0-mm size fraction (Harrison et al., unpublished data). All four models were allowed to vote in an ensemble; if either a majority of the classifiers voted for one classification with an average softmax value of over 0.8, the grain was marked as belonging to that classification. These thresholds were chosen based on the Jaccard scores between the human annotators involved in training the classifiers. If neither condition was met, the grain was classified as 'other'. Silt-clay lumps, which were an artifact of the high drying heat, were excluded from further analyses. Bivalve, gastropod and unidentified mollusc were merged into 'Mollusc', bringing the total number of output classes to seven: bryozoan, calcareous algae, coral, echinoderm, foraminifera, mollusc and other.

2.6 | Pipeline building

Following training and testing, the SAND-e pipeline was put to work. Once the inference model for both the 'Segmentation' and 'Classification' tasks was extracted, all images from the dataset could be run through each stage. Images were first passed through the segmenter code, using JSON (Pezoa et al., 2016) and NumPy (Harris et al., 2020) libraries in Python, loading each image and passing it through an OpenVINO (Demidovskij et al., 2019) model. This process locates grains, crops around each boundary from the background versus the grain, and outputs each grain as an individual .png file. Subsequently, all individual grain files are run through the classifier code, which uses a softmax layer to give the most probable classification label for each grain and associates a confidence level

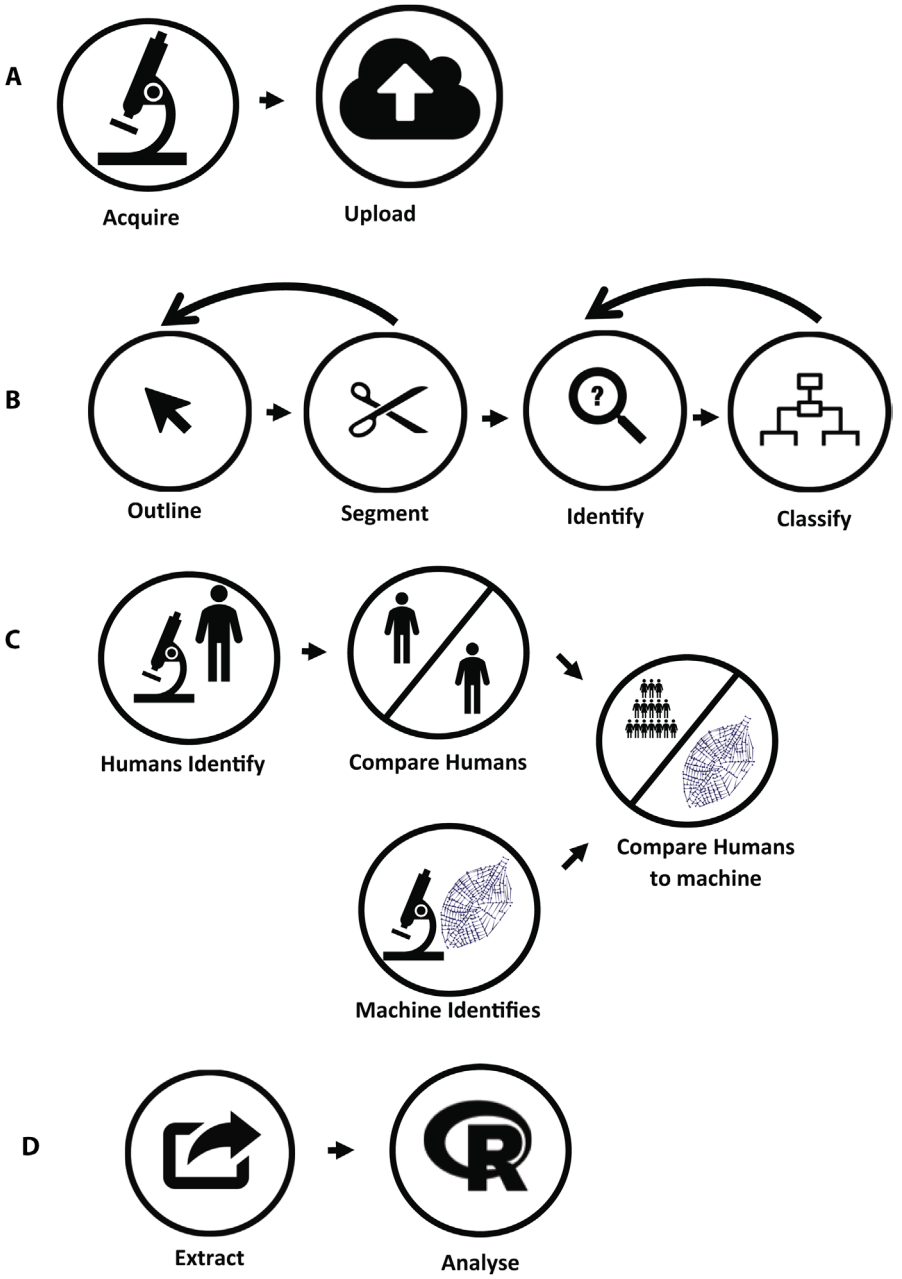

FIGURE 2 Schematic workflow demonstrating the three phases of methodological approaches carried out towards the aims of the project between October and December 2021 where (A) data collection and preparation, (B) model training, (C) model testing and (D) analyses.

to each. The output of the classifier is a file with classifications predicted for each grain, the confidence of each prediction and the filename of each grain for sense checking. All four classifiers were run on all grains, producing four output files. Those files were then loaded into an R script where the classifier ensemble voted. All Python and R scripts required to run SAND-e locally are provided on Github.

2.7 | Testing

While the internal testing offered preliminary precision and recall values for the sanitised dataset provided to Geti for training, these metrics held no practical utility for real-world scenarios. Practical testing required comparing the output of the models against that of humans on unsorted samples that were not included in the training dataset (Figure 2C). The segmenter was tested by taking one image from each of the two size fractions of all nine sites, following the same procedures used to generate training data. The images were then run through the segmenter, and the resulting segmented images were compared to the manually identified grains. To test the comparability of the classifier ensemble and humans, 10 humans who are experts in sedimentology or experts in at least one of the grain types were asked to annotate the grains from the segmenter test. The humans were given the same set of 18 images with the numbered grains generated in the segmenter test. The classification

algorithms were then run on the smaller files produced by the segmenter from the original 18 images; the three ensembles were allowed to vote, and their votes were compared to the human results using Jaccard Indices and Cohen's Kappa Coefficients; hierarchical clustering and PERMANOVA tests were performed to detect differences in error rates. Jaccard indices were chosen due to their similarity to traditional methods of comparing percent agreement between human instructors and students, allowing for comparison between current methodologies and the new methodology proposed here. Cohen's kappa coefficients ensure that rarer classes are annotated correctly, unlike the Jaccard scores which can be biased if the model performs well on common classes but not rare ones. SAND-e failed to classify echinoderms at a human level; thus they were excluded from further analyses.

2.8 | Deployment

All 1676 images were run through the segmenter and the results were fed into all four classifiers (Figure 2D). Silt-clay lumps, which were an artefact of the high temperatures used for drying the samples, were retained for model testing but excluded from environmental analysis. Statistical analyses were performed with the R-statistical software (R Core Team, 2021). PERMANOVA tests were run in the vegan package (Oksanen et al., 2022) using Bray–Curtis dissimilarities to test the a priori hypothesis that sediment composition varied significantly between reefs and/or size fractions. Additionally, hierarchical clustering was run to find clusters beyond the a priori hypotheses, while principal component analyses from the vegan package (Oksanen et al., 2022) were used to visualise these clusters. A schematic workflow is provided to elucidate the processes described above (Figure 2).

3 | RESULTS

3.1 | Light Availability

Triangle Reef has half of the midday light availability in comparison to Blue Lagoon (Figure 3), placing it almost exactly halfway between Blue Lagoon and Sakar North (Rosedy et al., 2023).

3.2 | Testing

During testing, the segmenter recovered 333 grains, including all 324 grains identified by the humans but also a few additional objects, including specks of dust and tiny sand grains that humans generally did not annotate. This is equal to a 2.8% difference. All grains identified by SAND-e but not by humans were labelled 'other' by the classifier ensemble. Due to the high success rate of the segmenter, further testing was not conducted.

By contrast, the classifier was tested more rigorously. Jaccard Indices and Cohen's Kappa Coefficients were calculated among all human annotators and between all humans and SAND-e. The Jaccard scores comparing SAND-e to human annotators were not significantly different from the inter-human annotator scores, albeit on the lower end.

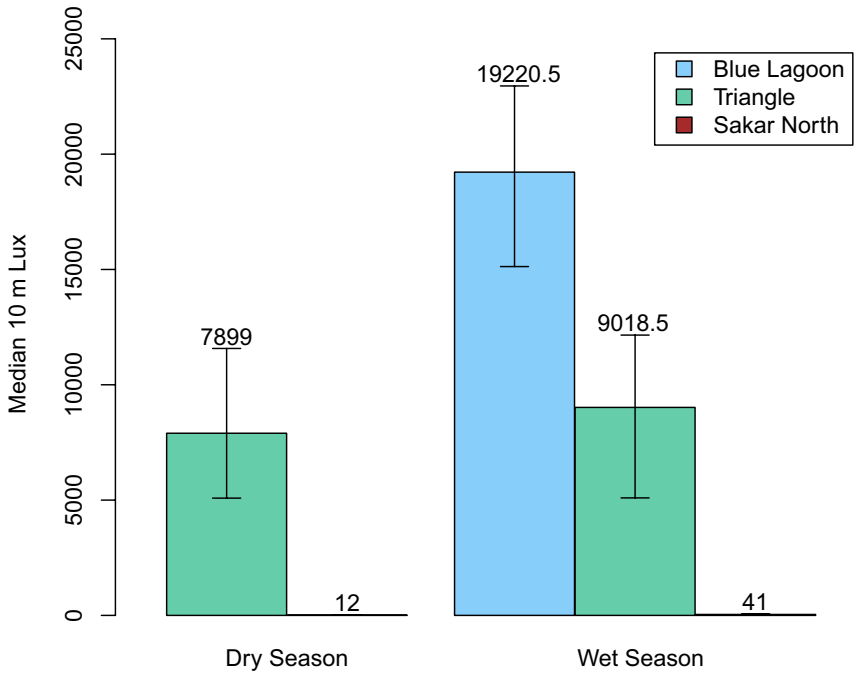

FIGURE 3 Median light levels, expressed as LUX, measured at mid-day at 10 m depth at Blue Lagoon and Sakar North. Measurements were taken every 5 minutes by in situ dataloggers over a period from October to November for the dry season and June for the wet season. All data was logged in 2019, which is the year sediment samples were taken.

SAND-e performed within the range of human error on all classes except echinoderms, so echinoderms were excluded from further analyses. Not enough bryozoans were present in the test dataset to make the results statistically significant, so they were also excluded. Precision, recall, F-score and confusion matrices are available as appendices.

3.3 | Deployment

When deployed on the full dataset, a total of 32 883 grains were obtained from the 1676 images run through the segmenter model and subsequently classified. Segmentation, Classification, and voting together took 1 hour. Of the 32 883 grains identified, 7409 (23%) were identified by the ensemble; the remaining 25 495 (77%) were either in the 'other' class (98.1%) or identified as bryozoan (0.1%) or echinoderm (1.8%), and therefore excluded. Differences in sediment producer contributions to the two size fractions used in this study were on the edge of significance (df = 17, $R^2 = 0.18$, $F = 3.57$, $p = 0.054$). Significant differences were found between the sediments in Blue Lagoon, Triangle, and Sakar North (df = 8, $R^2 = 0.91$, $F = 29.61$, $p = 0.003$, Figures 4 and 5) and in both the 0.5–1.0 mm (df = 8, $R^2 = 0.78$, $F = 10.90$, $p = 0.006$) and 1.0–1.4 mm (df = 8, $R^2 = 0.90$, $F = 26.38$, $p = 0.005$) size fractions.

4 | DISCUSSION

The segmenter was fast and made virtually no errors relative to humans. Furthermore, segmentation was fully automated and did not require any human input, making it more efficient than one-click segmenters, such as those based on the Segment Anything model (Sylvester, 2023). In general, the classifier ensemble scored lower than the general sediment experts but equal to the people who specialise in only one taxon, especially if that taxon

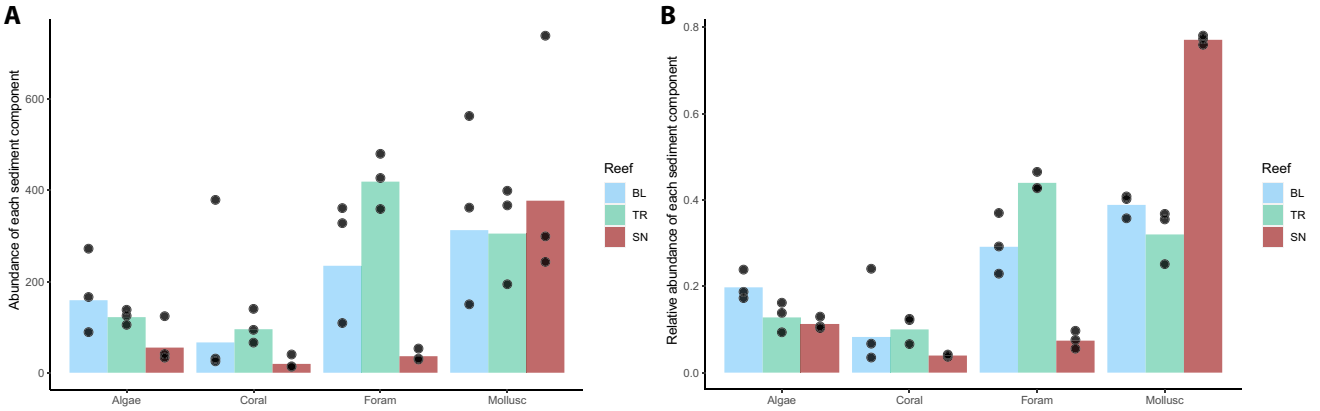

FIGURE 4 Bar charts showing the (A) raw abundances and (B) percent abundances of surveyed grains. Dots represent the three replicate samples per site and bars represent the geometric mean of those three.

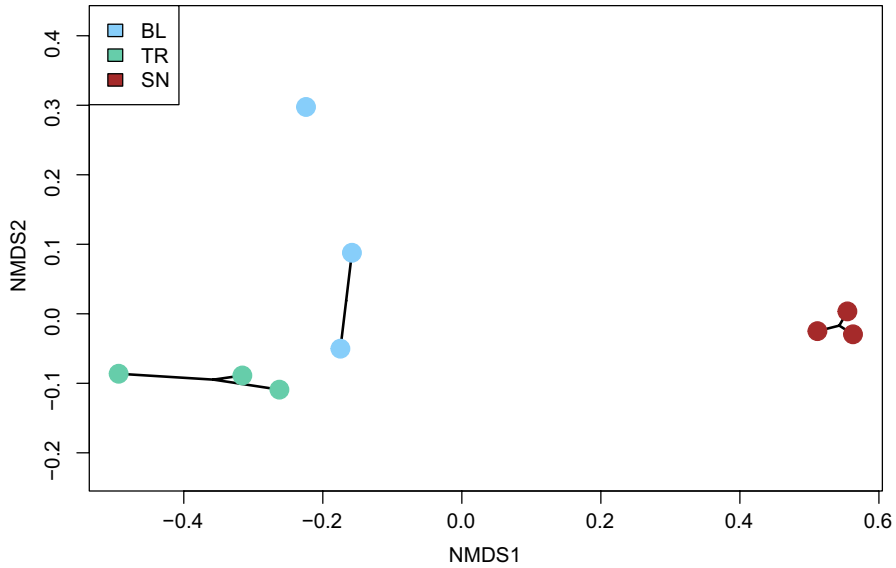

FIGURE 5 NMDS of the results from SAND-e with hierarchical clustering. Point colour represents the site, point shape denotes the size fraction and the lines between points are determined by hierarchical clustering.

was rare in the dataset (Table 2). Furthermore, the errors were spread evenly across classes; SAND-e identified all components within the range of values produced by human annotators (Figure 6A,B, supplemental material), both including 'other' grains (Figure 6A) and excluding them (Figure 6B). Additionally, the ecological environment recovered by the NMDS analyses was within the range of human annotators (Figure 6C) and was only significantly different from three of the eleven humans (Table 3). Hierarchical clustering placed SAND-e's Jaccard scores within the error rate of expert human sedimentologists, albeit at the lower end (Figure 6D). These human-comparable rates of error indicate that SAND-e is ready for deployment. The fact that these models could function well even on sediments from the Triangle Reef, on which they were not at all trained, suggests that they possess some generalisability. Future projects will require testing and possibly retraining the classifiers to increase functionality to other sites and geographic regions. Classifiers for specific groups of sediment producers, such as foraminifera (Marchant et al., 2020) or ichthyoliths (Mimura et al., 2022), are becoming more common, but no one has yet attempted to create a coarse sediment classification system. In theory, SAND-e could serve as a starting point that other researchers use to isolate the component they are studying (e.g. foraminifera) and feed SAND-e's outputs into a more specialised classifier of their design. Machine-learning powered robotic sorters for insects, meiofauna and other small samples are already in development; if one could be modified to accept sediment then SAND-e's fast-running MaskRCNN-ResNet50 and EfficientNet models could be deployed as a preliminary sorting step, in which sieved sand would be inserted and taxa of interest would be automatically picked from the sediment. Even with the crude classification level provided by SAND-e, the signal of sediment producers showed great variation between reefs. Blue Lagoon, the clear-water reef, showed by far the most abundant calcareous algae contents, which were the only exclusive autotrophs prevalent in this study. There, mixotrophic foraminifers and symbiotic corals contributed in equal proportions to the sediment as heterotrophic mollusks. In the Triangle Reef, at mid-levels of turbidity, mixotrophic foraminifera and corals were dominant, with mollusks coming in second place as sediment producers and algae trailing in third. In contrast, Sakar North reef, with the highest turbidity, had a strong mollusk dominance and a lower abundance of forams and corals. A high abundance of mollusks has been reported from other turbid reefs (Bonesso et al., 2022; Janßen et al., 2017) though not with as high values as in Sakar North. The significant differences in the distribution of trophic types of

TABLE 2 Jaccard scores and Cohen's kappa coefficients for SAND-e and 11 human annotators. Jaccard scores are found on the top right portion of the table while Cohen's kappa coefficients are on the bottom right. Jaccard scores were chosen due to their similarity to traditional methods of comparing percent agreement between human instructors and students, allowing for comparison between current methodologies and the new methodology proposed here. Cohen's kappa coefficients ensure that rarer classes are annotated correctly, unlike the Jaccard scores which can be biased if the model performs well on common classes but not rare ones.

	SAND-e	Human 1	Human 2	Human 3	Human 4	Human 5	Human 6	Human 7	Human 8	Human 9	Human 10	Human 11
SAND-e		0.73	0.69	0.69	0.70	0.69	0.71	0.71	0.63	0.77	0.61	0.79
Human 1	0.50		0.79	0.83	0.82	0.80	0.78	0.82	0.65	0.89	0.73	0.90
Human 2	0.48	0.64		0.77	0.80	0.76	0.74	0.80	0.70	0.78	0.71	0.81
Human 3	0.46	0.69	0.63		0.78	0.82	0.73	0.79	0.68	0.81	0.70	0.84
Human 4	0.50	0.68	0.68	0.64		0.79	0.77	0.82	0.73	0.82	0.72	0.84
Human 5	0.48	0.66	0.62	0.70	0.66		0.78	0.70	0.71	0.80	0.69	0.82
Human 6	0.48	0.59	0.57	0.55	0.61	0.63		0.75	0.69	0.78	0.68	0.79
Human 7	0.50	0.68	0.67	0.66	0.71	0.68	0.59		0.67	0.82	0.75	0.83
Human 8	0.44	0.47	0.57	0.54	0.59	0.57	0.54	0.52		0.68	0.62	0.67
Human 9	0.56	0.77	0.63	0.64	0.68	0.64	0.59	0.68	0.51		0.73	0.89
Human 10	0.36	0.54	0.55	0.53	0.56	0.52	0.48	0.61	0.44	0.54		0.73
Human 11	0.59	0.80	0.66	0.70	0.71	0.67	0.60	0.70	0.50	0.77	0.55	

Note: Green shows values between 1.0–0.7 for Jaccard indices and 1.0–0.6 for Kohen's Kappa Coefficients. Orange shows values between 0.7–0.5 for Jaccard indices and 0.6–0.4 for Kohen's Kappa Coefficients. Red shows values under 0.5 for Jaccard indices and 0.4 for Kohen's Kappa Coefficients.

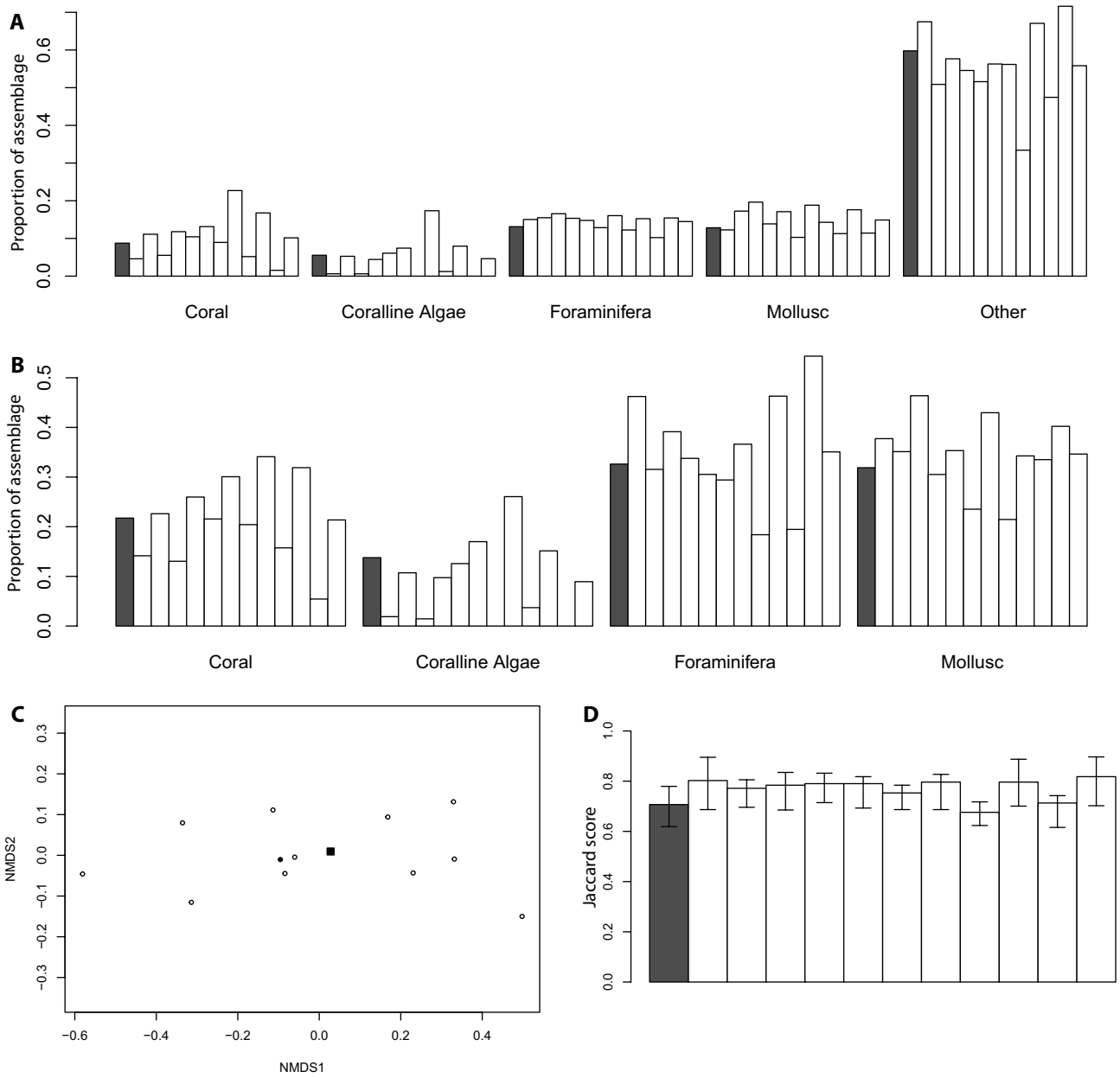

FIGURE 6 Results of classification by SAND-e in grey and the human annotators in white with (A) and without (B) other grains. (C) NMDS of results from SAND-e and human annotators. SAND-e is displayed with a filled circle while human annotators are shown with empty circles. The average of all human annotators is shown with a square. (D) Jaccard scores of SAND-e (grey) and 11 human annotators (white).

sediment producers suggest that sedimentology might be influenced by environmental factors. Further studies are needed to test this initial trend, particularly on turbid reefs, to better understand how they function on a sedimentological level.

These preliminary results demonstrate the utility of SAND-e for sedimentologists. Rapid, crude classification of sediments can assist sedimentologists in many different analyses. Allowing sedimentologists to utilise replicates is one pressing utility. Sediment from Blue Lagoon's samples differed significantly despite the samples being collected within 10 meters of each other. This is noteworthy since most studies on intra-reef variation take samples at 50–100 m intervals on the assumption that small-scale variation is negligible (Bonesso et al., 2022; Kappelmann et al., 2023). SAND-e's rapid, crude classification of sediment would allow studies of replicates taken near each other to elucidate the scale on which sedimentological variation occurs on coral reefs. If future studies confirm that significant variation occurs on scales smaller than traditional sampling intervals, SAND-e can allow sedimentologists to include metre-scale replicates

TABLE 3 *T* statistics, degrees of freedom, and *p*-values comparing SAND-e's performance to all 11 humans.

	T-stat	df	*p*-value
Human 1	−2.16	22	0.041
Human 2	−1.43	21	0.166
Human 3	−1.58	22	0.126
Human 4	−2.01	21	0.057
Human 5	−1.66	21	0.112
Human 6	−1.06	21	0.299
Human 7	−1.87	21	0.075
Human 8	0.62	22	0.541
Human 9	−2.27	21	0.034
Human 10	0.10	22	0.91
Human 11	−2.65	21	0.015

in their surveys without increasing the time costs of projects, allowing sedimentologists to distinguish between large-scale trends in sediment composition and metre-scale noise. Similarly, reef cores can be sampled at more frequent intervals, allowing researchers a clearer view of how sediments changed over time and helping distinguish gradual changes from rapid shifts. Island formation analyses, sediment transport studies, paleoecological reconstructions and reef health studies are among the many uses of coral reef sediment that would benefit from increased data with consistent errors generated by SAND-e.

Despite its benefits, SAND-e has several major drawbacks over traditional sedimentological methods. Firstly, SAND-e works on images and therefore requires researchers to have access to a photo-microscope. While training data was acquired on multiple microscopes with different lighting conditions, SAND-e still requires reasonably sharp images with decent lighting. Secondly, the current version of SAND-e's segmenter requires grains to be spread out; by contrast, most sedimentologists who work from photographs of sediment use filled trays. Separating the grains requires extra time input. That being said, it is still faster than traditional methods and the photography step can be conducted by volunteers with limited training, unlike traditional picking, which requires all steps to be conducted by an expert. Future versions of SAND-e will either focus on improving the segmenter to handle touching grains or will partner with an existing segmenter that can already accomplish this. Thirdly, SAND-e is only trained on grains between 2 mm and 0.5 mm. Sediment components are known to vary depending on the size of the fractions used for the analyses (Hausmann et al., 2018). Smaller and larger size fractions will contain grains that are not in its training data (e.g. small, heterotrophic foraminifera; large coral fragments) which it will not be able to classify reliably. Future iterations of SAND-e will seek to add smaller size fractions to its dataset, which will expand its applicability and make it more useful across a broader range of sediment samples. Additionally, SAND-e is unable to physically manipulate the sediment it processes so it cannot return sorted sediment for weighing, isotope analyses or other uses. Future work will include creating or acquiring a sediment picking robot to allow SAND-e to physically pick sediments. Furthermore, it is useful to remember that the 'other' category is not a class on which SAND-e was trained but rather a tag given to any grain that does not have a high enough softmax value to be classified. As such, grains may be incorrectly labelled as 'other' if they are too poorly preserved for SAND-e to classify them.

5 | CONCLUSIONS

SAND-e represents the first machine learning pipeline capable of automatically segmenting carbonate sand from images and classifying the producers of each individual component on a coarse scale. Its framework is flexible by design, allowing the models to be swapped out and re-trained as well as making it simple to add new classes as needed by future projects. We expect the use of machine learning in sedimentological workflows to boost the speed and comparability of experiments, allowing sedimentologists to process larger datasets than were possible under traditional manual classification methods.

ACKNOWLEDGEMENTS

This study is part of the Reef Refugia project (NE/R011044/1) funded by NERC. We would like to acknowledge the support and assistance from Sindia Sosdian (Cardiff Uni.), Chris Perry (Exeter Uni.), Natasha Senior (NHM, ZSL), Liz Wood, Dominic Monteroso (Darvel Bay Diving Centre), Indra Van Oppen (Tropical Research and Conservation Centre), Tina van de Flierdt, Martin Blunt (Earth Science Dept, Imperial College London), Fisheries Department Malaysia and ESSCOM. We acknowledge Sabah Biodiversity Centre as the access licence holder JKM/MBS.1000-2/2 JLD.7(161) and the Economic Planning Unit, Ministry of Economic Affairs of Malaysia for granting the Research Permit UPE 40/200/193533. NS and TC thank the core imaging labs at the NHM for SEM imagery. AR thanks the Higher Education Funding Council for Wales (HEFCW) and the GCRF for funding and remote-training internship at NHM and Cardiff University. AR thanks Universiti Malaysia Sabah for partially funding this field work in tandem with the 'Dynamics of marginal coral reef ecosystems in Semporna' project under the Skim

Geran Bantuan Penyelidikan Pascasizwazah (UMSGreat) grant (GUG0415-2/2019). WH, WR and KJ thank the 4D-REEF project funded by the European Union's Horizon 2020 research and innovation programme under the Marie Sklodowska-Curie grant agreement No 813360. We thank all the humans who helped generate the testing dataset. We thank Tempcon for partial sponsorship of Hobos. WH thanks Laurens Hogeweg (Naturalis Biodiversity Center) and Christine Dönszelmann for helping with the python coding.

DATA AVAILABILITY STATEMENT

The models, Python environment and code required to run SAND-e locally will be shared publicly on Github with version control upon publication. The training data for SAND-e will be shared in an image archive upon publication. The raw data and code from this study will be shared upon publication.

ORCID

G. William M. Harrison https://orcid.org/0000-0002-2563-7695
Nadia Santodomingo https://orcid.org/0000-0003-1392-2672
Willem Renema https://orcid.org/0000-0002-1627-5995

REFERENCES

Anthony, K.R.N., Connolly, S.R. & Hoegh-Guldberg, O. (2007) Bleaching, energetics, and coral mortality risk: effects of temperature, light, and sediment regime. *Limnology and Oceanography*, 52, 716–726.

Bonesso, J.L., Browne, N.K., Murley, M., Dee, S., Cuttler, M.V.W., Paumard, V., Benson, D. & O'Leary, M. (2022) Reef to Island sediment connections within an inshore turbid reef Island system of the eastern Indian Ocean. *Sedimentary Geology*, 436, 106177. https://doi.org/10.1016/j.sedgeo.2022.106177

Brown, K.T., Bender-Champ, D., Achlatis, M., van der Zande, R.M., Kubicek, A., Martin, S.B., Castro-Sanguino, C., Dove, S.G. & Hoegh-Guldberg, O. (2021) Habitat-specific biogenic production and erosion influences net framework and sediment coral reef carbonate budgets. *Limnology and Oceanography*, 66, 349–365. https://doi.org/10.1002/lno.11609

Buscombe, D. (2020) SediNet: a configurable deep learning model for mixed qualitative and quantitative optical granulometry. *Earth Surface Processes and Landforms*, 45, 638–651. https://doi.org/10.1002/esp.4760

Butler, J.B., Lane, S.N. & Chandler, J.H. (2001) Automated extraction of grain-size data from gravel surfaces using digital image processing. *Journal of Hydraulic Research*, 39(5), 519–529. https://doi.org/10.1080/00221686.2001.9628276

Cramer, K., O'Dea, A., Clark, T., Zhao, J.-X. & Norris, R.D. (2017) Prehistorical and historical declines in Caribbean coral reef accretion rates driven by loss of parrotfish. *Nature Communications*, 8, 14160. https://doi.org/10.1038/ncomms14160

Cuttler, M.V.W., Hansen, J.E., Lowe, R.J., Trotter, J.A. & McCulloch, M.T. (2019) Source and supply of sediment to a shoreline salient in a fringing reef environment. *Earth Surface Processes and Landforms*, 44, 552–564. https://doi.org/10.1002/esp.4516

De'ath, G., Lough, J.M. & Fabricius, K.E. (2009) Declining coral calcification on the Great Barrier Reef. *Science*, 323(5910), 116–119.

Demidovskij, A., Gorbachev, Y., Fedorov, M., Slavutin, I., Tugarev, A., Fatekhov, M. & Tarkan, Y. (2019) OpenVINO deep learning workbench: Comprehensive analysis and tuning of neural networks inference. In: *Proceedings of the IEEE International Conference on Computer Vision Workshops*. Seoul, Korea: IEEE.

Guest, J.R., Baird, A.H., Maynard, J.A., Muttaqin, E., Edwards, A.J., Campbell, S.J., Yewdall, K., Affendi, Y.A. & Chou, L.M. (2012) Contrasting patterns of coral bleaching susceptibility in 2010 suggest an adaptive response to thermal stress. *PLoS One*, 7, e33353. https://doi.org/10.1371/journal.pone.0033353

Harris, C.R., Millman, K.J., van der Walt, S.J., Gommers, R., Virtanen, P., Cournapeau, D., Wieser, E., Taylor, J., Berg, S., Smith, N.J., Kern, R., Picus, M., van Hoyer, S., Kerkwijk, M.H., Brett, M., Haldane, A., Fernández del Río, J., Wiebe, M., Peterson, P., Gérard-Marchant, P., Sheppard, K., Reddy, T., Weckesser, W., Abbasi, H., Gohlke, C. & Oliphant, T. (2020) Array programming with NumPy. *Nature*, 585, 357–362. https://doi.org/10.1038/s41586-020-2649-2

Hausmann, I.M., Domanski, H. & Zuschin, M. (2018) Influence of setting, sieve size, and sediment depth on multivariate and univariate assemblage attributes of coral reef-associated mollusc death assemblages from the Gulf of Aqaba. *Facies*, 64, 20. https://doi.org/10.1007/s10347-018-0530-7

Hoegh-Guldberg, O. (1999) Climate change, coral bleaching and the future of the world's coral reefs. *Marine and Freshwater Research*, 50, 839–866.

Janßen, A., Wizemann, A., Klicpera, A., Satari, D.Y., Westphal, H. & Mann, T. (2017) Sediment composition and facies of coral reef islands in the Spermonde Archipelago, Indonesia. *Frontiers in Marine Science*, 4(144). https://doi.org/10.3389/fmars.2017.00144

Jin, Z., Azzari, G., You, C., Di Tommaso, S., Aston, S., Burke, M. & Lobell, D.B. (2019) Smallholder maize area and yield mapping at national scales with Google Earth Engine. *Remote Sensing of Environment*, 228, 115–128. https://doi.org/10.1016/j.rse.2019.04.016

Johnson, J.A., Perry, C.T., Smithers, S.G., Morgan, K.M., Santodomingo, N. & Johnson, K.G. (2017) Palaeoecological records of coral community development on a turbid, nearshore reef complex: baselines for assessing ecological change. *Coral Reefs*, 36, 685–700. https://doi.org/10.1007/s00338-017-1561-1

Kappelmann, Y., Westphal, H., Kneer, D., Wu, H.C., Wizemann, A., Jompa, J. & Mann, T. (2023) Fluctuating sea-level and reversing Monsoon winds drive Holocene lagoon infill in Southeast Asia. *Scientific Reports*, 13(5042). https://doi.org/10.1038/s41598-023-31976-z

Kosnik, M.A., Hua, Q., Kaufman, D.S. & Wüst, R.A. (2009) Taphonomic bias and time-averaging in tropical molluscan death assemblages: differential shell half-lives in Great Barrier

Reef sediment. *Paleobiology*, 35(4), 565–586. https://doi.org/10.1666/0094-8373-35.4.565

Lange, I.D., Razak, T.B., Perry, C.T., Maulana, P.B., Prasetya, M.E., Irwan & Lamon, T.A.C. (2024) Coral restoration can drive rapid reef carbonate budget recovery. *Current Biology*, 34(6), 1341–1348. https://doi.org/10.1016/j.cub.2024.02.009

Laux, A., Waltert, M. & Gottschalk, E. (2022) Camera trap data suggest uneven predation risk across vegetation types in a mixed farmland landscape. *Ecology and Evolution*, 12, 9027. https://doi.org/10.1002/ece3.9027

Lürig, M.D., Donoughe, S., Svensson, E.I., Porto, A. & Tsuboi, M. (2021) Computer vision, machine learning, and the promise of phenomics in ecology and evolutionary biology. *Frontiers in Ecology and Evolution*, 9. https://doi.org/10.3389/fevo.2021.642774

Mair, D., Witz, G., Do Prado, A.H., Garefalakis, P. & Schlunegger, F. (2024) Automated detecting, segmenting and measuring of grains in images of fluvial sediments: the potential for large and precise data from specialist deep learning models and transfer learning. *Earth Surface Processes and Landforms*, 49(3), 1099–1116. https://doi.org/10.1002/esp.5755

Marchant, R., Tetard, M., Pratiwi, A., Adebayo, M. & de Garidel-Thoron, T. (2020) Automated analysis of foraminifera fossil records by image classification using a convolutional neural network. *Journal of Micropalaeontology*, 39, 183–202. https://doi.org/10.5194/jm-39-183-2020

McKoy, H., Kennedy, D.M. & Kench, P.S. (2010) Sand cay evolution on reef platforms, Mamanuca Islands, Fiji. *Marine Geology*, 269(1–2), 61–73.

Mimura, K., Minabe, S., Nakamura, K., Yasukawa, K., Ohta, J. & Kato, Y. (2022) Automated detection of microfossil fish teeth from slide images using combined deep learning models. *Applied Computing and Geosciences*, 16(100092), 100092. https://doi.org/10.1016/j.acags.2022.100092

Moberg, F. & Folke, C. (1999) Ecological goods and services of coral reef ecosystems. *Ecological Economics*, 29(2), 215–233. https://doi.org/10.1016/S0921-8009(99)00009-9

Morgan, K.M. & Kench, P.S. (2016) Reef to Island sediment connections on a Maldivian carbonate platform: using benthic ecology and biosedimentary depositional facies to examine Island-building potential. *Earth Surface Processes and Landforms*, 41, 1815–1825. https://doi.org/10.1002/esp.3946

Morgan, K.M., Perry, C.T., Johnson, J.A. & Smithers, S.G. (2017) Nearshore turbid-zone corals exhibit high bleaching tolerance on the Great Barrier Reef following the 2016 ocean warming event. *Frontiers in Marine Science*, 4. https://doi.org/10.3389/fmars.2017.00224

O'Dea, A., Lepore, M., Altieri, A.H., Chan, M., Morales-Saldaña, J.M., Muñoz, N.-H., Pandolfi, J.M., Toscano, M.A., Zhao, J.-x. & Dillon, E.M. (2020) Defining variation in pre-human ecosystems can guide conservation: an example from a Caribbean coral reef. *Scientific Reports*, 10, 2922. https://doi.org/10.1038/s41598-020-59436-y

Oksanen, J., Simpson, G., Blanchet, F., Kindt, R., Legendre, P., Minchin, P., O'Hara, R., Solymos, P., Stevens, M., Szoecs, E., Wagner, H., Barbour, M., Bedward, M., Bolker, B., Borcard, D., Carvalho, G., Chirico, M., De Caceres, M., Durand, S., Evangelista, H., FitzJohn, R., Friendly, M., Furneaux, B., Hannigan, G., Hill, M., Lahti, L., McGlinn, D., Ouellette, M., Ribeiro Cunha, E., Smith, T., Stier, A., Ter Braak, C. & Weedon, J. (2022) vegan: community ecology package_. R package version 2.6-4. https://CRAN.R-project.org/package=vegan

Perry, C.T., Lange, I. & Januchowski-Hartley, F.A. (2018) ReefBudget Indo Pacific: online resource and methodology. Retrieved from http://geography.exeter.ac.uk/reefbudget/

Perry, C.T., Lange, I.D. & Stuhr, M. (2023) Quantifying reef-derived sediment generation: introducing the SedBudget methodology to support tropical coastline and Island vulnerability studies. *Cambridge Prisms: Coastal Futures*, 1(26). https://doi.org/10.1017/cft.2023.14

Pezoa, F., Reutter, J.L., Suarez, F., Ugarte, M. & Vrgoč, D. (2016) 'Foundations of JSON schema', 25th International World Wide Web Conference, WWW 2016 (International World Wide Web Conferences Steering Committee), pp. 263–273. https://doi.org/10.1145/2872427.2883029

Porto, A. & Voje, K.L. (2020) ML-morph: a fast, accurate and general approach for automated detection and landmarking of biological structures in images. *Methods in Ecology and Evolution*, 11, 500–512. https://doi.org/10.1111/2041-210X.13373

R Core Team. (2021) *R: A language and environment for statistical computing*. Vienna: R Foundation for Statistical Computing. Available from: https://www.R-project.org/ [Accessed January 10, 2022].

Roelfsema, C.M., Joyce, K.E. & Phinn, S.R. (2006) Evaluation of benthic survey techniques for validating remotely sensed images of coral reefs. Proceedings of the 10th International Coral Reefs Symposium, 1, pp. 1771–1780.

Rosedy, A., Ives, I., Waheed, Z., Hussein, M.A.S., Sosdian, S., Johnson, K.G. & Santodomingo, N. (2023) Turbid reefs experience lower coral bleaching effects in NE Borneo (Sabah, Malaysia). *Regional Studies in Marine Science*, 68, 103268.

Santodomingo, N., Renema, W. & Johnson, K.G. (2016) Understanding the murky history of the Coral Triangle: Miocene corals and reef habitats in East Kalimantan (Indonesia). *Coral Reefs*, 35, 765–781. https://doi.org/10.1007/s00338-016-1427-y

Sinha, A. & Abernathey, R. (2021) Estimating ocean surface currents with machine learning. *Frontiers in Marine Science*, 8. https://doi.org/10.3389/fmars.2021.672477

Sylvester, Z. (2023) Segment every grain. https://github.com/zsylvester/segmenteverygrain [Accessed December 8th, 2023]

The Intel® Geti™ Platform. (2023) The Intel® Geti™ Platform [computer software]. Version 1.5.0. https://geti.intel.com/

Woodroffe, C.D. & Morrison, R.J. (2001) Reef-Island accretion and soil development on Makin, Kiribati, central Pacific. *Catena*, 44(4), 245–261. https://doi.org/10.1016/S0341-8162(01)00135-7

Woodroffe, C.D., Samosorn, B., Hua, Q. & Hart, D.E. (2007) Incremental accretion of a sandy reef Island over the past 3000 years indicated by component-specific radiocarbon dating. *Geophysical Research Letters*, 34, L03602. https://doi.org/10.1029/2006GL028875

Zuschin, M., Hohenegger, J. & Steininger, F.F. (2000) A comparison of living and dead molluscs on coral reef associated hard substrata in the northern Red Sea—implications for the fossil

record. *Palaeogeography, Palaeoclimatology, Palaeoecology*, 159(1–2), 167–190. https://doi.org/10.1016/S0031-0182(00)00045-6

Zweifler, A., Dee, S. & Browne, N.K. (2024) Resilience of turbid coral communities to marine heatwave. *Coral Reefs*, 43, 1303–1315. https://doi.org/10.1007/s00338-024-02538-0

SUPPORTING INFORMATION

Additional supporting information can be found online in the Supporting Information section at the end of this article.

How to cite this article: Harrison, G.W.M., Collins, T.G., Rosedy, A., Santodomingo, N., Renema, W. & Johnson, K.G. (2025) Taking machine learning with a grain of sand: Sediment Analysis Neural-network Data-engine (SAND-e) reveals sedimentological differences between turbid and clear-water reefs. *The Depositional Record*, 00, 1–14. Available from: https://doi.org/10.1002/dep2.70051